

Genomic Expression Discovery Predicts Pathways and Opposing Functions behind Phenotypes*[§]

Received for publication, March 19, 2003
Published, JBC Papers in Press, April 16, 2003, DOI 10.1074/jbc.M302800200

Hassan M. Fathallah-Shaykh^{‡,§}, Bin He[‡], Li-Juan Zhao[‡], Herbert H. Engelhard[¶],
Leonard Cerullo^{||}, Terry Lichtor^{**}, Richard Byrne^{||}, Lorenzo Munoz^{||}, Kelvin Von Roenn^{||},
Gail L. Rosseau^{||}, Roberta Glick^{**}, Chen Sherman[‡], and Khan Farooq[‡]

From the Departments of [‡]Neurological Sciences and ^{||}Neurosurgery, Rush Presbyterian-St. Luke's Medical Center, Chicago, Illinois 60612, the [¶]Department of Neurosurgery, the University of Illinois at Chicago, Chicago, Illinois 60612, and the ^{**}Department of Neurosurgery, Cook County Hospital, Chicago, Illinois 60612

Discovering states of genetic expression that are true to a high degree of certainty is likely to predict gene function behind biological phenotypes. The states of expression (up- or down-regulated) of 19,200 cDNAs in 10 meningiomas are compared with normal brain by an algorithm that detects only 1 false measurement per 192,000; 364 genes are discovered. The expression data accurately predict activation of signaling pathways and link gene function to specific phenotypes. Meningiomas appear to acquire aberrant phenotypes by disturbing the balanced expression of molecules that promote opposing functions. The findings expose interconnected genes and propose a role of genomic expression discovery in functional genomics of living systems.

The completion of the Human Genome Project combined with the development of microarray technology and recent advances in mathematical biology have set the stage for the genome-wide discovery of differential gene expression between any biological samples from any living system. The term discovery implies the extrapolation of data without the confound of pre-existing biases. This laboratory has developed a mathematical solution for discovering highly specific states of genetic expression between genetic samples (up- or down-regulated). The false discovery rate of the algorithm for microarrays that contain 19,200 cDNAs is $< 0.001\%$.¹ To explore the idea that genomic expression discovery predicts pathways and functions behind the biological phenotypes of living systems, we compare a tumor to its normal host organ. The expression data accurately predict activation of signaling pathways and propose that unbalanced opposing genetic functions create “aberrant” phenotypes. In addition, known molecular interactions reveal a rich network of stimulatory and inhibitory genetic interconnections.

We use microarrays containing 19,200 cDNAs to profile gene expression in 10 meningiomas *versus* normal brain. Meningiomas are compared with normal brain, its host organ, because

both tissue types contain non-tumor cells such as blood vessels and cells of lymphocytic lineage. Meningiomas comprise 15–20% of all primary intracranial tumors. They are abundantly vascular, tend to bleed during surgery, and often show ectopic calcification on computed tomographic (CT) scanning. Multiple meningiomas occur in association with a mutated neurofibromatosis type II tumor suppressor gene, known as merlin or schwannomin. Merlin protein appears to stabilize F-actin (2–4). Normal brain RNA was pooled from the occipital lobes of four individuals with no known neurological disease whose brains were frozen less than 3 h postmortem.

EXPERIMENTAL PROCEDURES

Reagents—Information on the antibodies used may be obtained from the corresponding web sites: anti- β -catenin, www.upstatebiotech.com; anti-glyceraldehydes-3-phosphate dehydrogenase (G3PDH), www.trevigen.com; anti-Akt,² anti-phospho-Akt (Ser-473), anti-p44/42 MAP kinase (ERK), and anti-phospho-p44/p42 Map kinase (Thr-202/Tyr-204, ERK-P), www.cellsignal.com.

Tumors—Patients signed informed consents, and the study is approved by the Institutional Review Boards of Rush University and Cook County Hospital. Tumor samples are frozen in liquid nitrogen in the operating room. The quality of RNA is assayed by gel electrophoresis; only high quality reference and sample RNAs are processed.

Microarray Experiments—All total RNA samples are analyzed in reference to a single standard obtained by pooling RNA from human occipital lobes. The latter are harvested and pooled from four individuals with no known neurological disease whose brains were frozen less than 3 h postmortem. Total RNA (5–10 μ g) is reverse-transcribed and the cDNA products labeled by the amino-allyl method with switching of probes between sample and reference and hybridized to 19K gene microarrays purchased from the Ontario Cancer Institute (www.microarrays.ca). Each 19K microarray consists of two slides containing a total of 38,400 spots representing 19,200 genes laid in duplicates (19,200 spots/slide). The 19K microarray slides are scanned at 10 μ m by a confocal scanner (Packard 4000XL, lifesciences.perkinelmer.com). Images are analyzed by Imagene software (www.biodiscovery.com).

RESULTS AND DISCUSSION

The results reveal that 364 genes are consistently up- or down-regulated in at least 5/10 meningiomas as compared with normal brain (Fig. 1). The genes and their differential expression are presented in Tables I–XI in supplementary information; 256 genes are either known or are ESTs homologous to known genes (Tables I–X S (supplement)). The remaining are uncharacterized ESTs (Table XI S). Tables I–VII S classify the genes based on how they may influence the biological chemistry of the cell. However, this grouping is not exclusive, because multifunctional genes belong to several classes.

* This work was supported by NCI, National Institutes of Health Grants R01-CA81367 and R29-CA78825 (to H. F.-S.) The costs of publication of this article were defrayed in part by the payment of page charges. This article must therefore be hereby marked “advertisement” in accordance with 18 U.S.C. Section 1734 solely to indicate this fact.

[§] The on-line version of this article (available at <http://www.jbc.org>) contains text and 11 Tables.

[§] To whom correspondence should be addressed: Rush University Medical Center, 2242 W. Harrison St., Suite 200, Chicago, IL 60612. Tel.: 312-563-3563; Fax: 312-563-3562; E-mail: hfathall@rush.edu.

¹ H. M. Fathallah-Shaykh, B. He, L.-J. Zhao, and A. Badruddin, submitted for publication.

² The abbreviations used are: Akt, protein kinase B; ERK, extracellular signal-regulated kinase; MAP, mitogen-activated protein; PI3K, phosphoinositide 3-kinase; EST, expressed sequence tag.

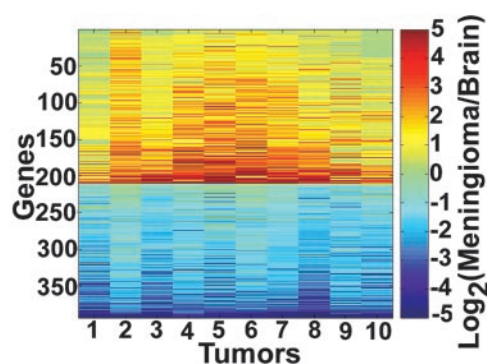


FIG. 1. Color representation of the expression data of 10 meningioma samples (columns) as compared with normal brain. To annul the effects of sample-to-sample variability in image quality in generating false negative data, we follow these steps in order to 1) apply the algorithm to find the genes differentially expressed in each tumor sample as compared with normal brain¹; 2) find the set of genes, *S*, that are extracted by the algorithm in at least one of the 10 tumors; and 3) identify the four “raw” replicate ratios of each of the genes of *S* in each tumor. We then apply a filter consisting of the following “fuzzy logic” rules in sequence. 1) All four replicate \log_2 (ratios) of a gene in any tumor are of the same sign and different from 0 (all four show either up- or down-regulation). 2) The mean of the four replicate ratios is either > 1.5 or < 0.67 . 3) If both rules 1 and 2 are true, compute the mean of the replicate \log_2 expression values; otherwise, exclude the genes by transforming the \log_2 expression to 0. 4) Exclude genes that are *not* resistant to both rules 1 and 2 in at least 5/10 tumors. And 5) exclude genes that are simultaneously up-regulated in one tumor and down-regulated in another. A total of 364 genes are discovered. cDNAs, spotted at several sites on a slide, are configured in multiple rows. Filtered measurements are represented by green. Positive (yellow to red) and negative (blue) \log_2 values indicate expression ratios higher than 1.5 and lower than 0.67, respectively.

The findings propose several hypotheses; elevated expression of dyskerin contributes to the previously reported telomerase activity in meningiomas (5). Loss of *Tho2* and higher expression of *PRKDC* are consistent with genomic instability (Table I S). As compared with normal brain, transcriptional activity is enhanced in meningiomas as evidenced by: 1) up-regulation of *PSIP2*, a transcriptional enhancer, 2) down-regulation of *NCOR2*, a transcriptional repressor, and 3) up-regulation of the transcription factors *TAF13*, *ZNRD1*, *MLL3*, *NET1*, and three zinc finger proteins (Table I S). Transcriptional activation is associated with enhanced expression of genes that regulate RNA processing, splicing, and degradation, including *WBP11*, *HNRPK*, *PCBP2*, and genes homologous to *tRNA* ligase and to *PAN2*. Enhanced transcriptional activity is also coupled with higher translational activity as evidenced by elevated expression levels of ribosomal proteins in meningiomas (Table I S).

Signaling pathways transmit information by phosphorylating specific proteins at specific sites. An assay that quantifies mRNA expression does not detect changes in protein phosphorylation; nevertheless, one expects microarrays to discover genes that are either targeted by the tumor or transcriptionally regulated when the signaling reaches the nucleus. Fig. 2a and Table II S show the differentially expressed genes related to the Wnt, MAP kinase, PI3K, and notch signaling and how they fit into the known molecular interactions of these pathways. The expression data reveal up-regulation of frizzles receptors, cyclin D1, and *IGF2* in meningiomas (Table II S). Activation of the up-regulated frizzles receptors is expected to lead to inhibition of *GSK3- β* , which causes accumulation of the β -catenin protein and its translocation to the nucleus where it induces the expression of cyclin D1 and *IGF2*. As predicted by the gene expression data (Fig. 2a), Western analysis confirms the activation of Wnt signaling as evidenced by significantly higher

amounts of the β -catenin protein in 11/18, and moderately increased amounts in 4/18 meningiomas as compared with normal brain (Fig. 2b). Loss of molecules that complex with protein kinase A (calmodulin 2, *PRKACB*, *AKAP6*, and *ITPR1*) and down-regulation of the 14–3–3 proteins (*YWHAH* and *YWHAH*) predict enhanced signaling through the MAP kinase and PI3K pathways. Moreover, the enhanced expression of *MKP1*, *TIMP3*, *MMP2*, *IRF1*, and *HNRPK* in meningiomas also implies activation of the MAP kinase pathway (Table II S). Here again, as predicted by the gene expression data, protein analysis confirms the activation of the MAP kinase and PI3K pathways as evidenced by phosphorylation of ERK (MAP kinase) and Akt (protein kinase B) in 7/7 and 12/18 meningiomas but not in normal brain, respectively (Fig. 2). Activation of both the MAP kinase and PI3K pathways enhances signaling through the notch pathway, which explains the elevated expression levels of *HES-1* and *Herp* in meningiomas (Table II S). Notch signaling is necessary to maintain the neoplastic phenotype in Ras-transformed human cells. G-proteins and G-protein-coupled receptors appear to play critical roles in signaling and growth. These include the molecules shown in Table II S that regulate signaling by controlling the intrinsic rate at which Ras, Rho, and Rab GTPases cycle between active GTP-bound and inactive GDP-bound states. In addition, *RGS4* (Table II S) hinders growth by inhibiting platelet-activating factor receptor phosphorylation.

Growth is enhanced by 1) the production of growth factors and their binding proteins, including *IGF2*, *IGFBP3*, *IGFBP4*, *IGFBP5*, *NOV*, and *CTGF* (Table III S); 2) the expression of the mitogenic receptors *CD14* and *LRP1*; and 3) the down-regulation of molecules that dampen signaling downstream from growth receptor activation, specifically, *RGS4* (Table II S), *PTPNS1*, *endophilin 1*, and *dynamain* (Table III S), which reduce receptor kinase-coupled signaling.

The cell cycle is deregulated in meningiomas. Cyclin D1, *E2F1*, *BTG2*, and *ID1*, which direct G_1/S transition, are up-regulated. *NET1*, which controls mitotic exit by anchoring the budding yeast regulator for nucleolar silencing and telophase complex to the nucleolus, is also up-regulated. Down-regulation of genes that arrest the cell cycle, including *CENPE*, *YWHAH*, and *YWHAH*, suggests deficient cell cycle control (Table II S). *CENPE* is required for establishing and maintaining a checkpoint that delays anaphase onset until all centromeres are correctly attached to the mitotic spindle. *YWHAH* and *YWHAH* belong to the 14–3–3 family of proteins that arrest the cell cycle at G_2 .

Transformation is induced by 1) enhanced expression of the oncogenes *ARNT*, *DSCR2*, *NET1*, *PTPN2*, *ID1*, and *MN1* (Table III S); 2) up-regulation of anti-apoptotic genes including *Herp*, *HES-1* (Table II S), and *S100A10* (p11, Table IV S); 3) down-regulation of the tumor suppressor genes *TU3A*, *PEG3*, and *C3ORF4* (Table III S); and 4) down-regulation of the pro-apoptotic genes *ITPR1* (Table II S), *ATP2B1* (Table IV S), *BNIP3*, and *BACH2* (Table IV S). In addition, molecules that interact with and modulate the effects of oncogenes and tumor suppressor genes are transcriptionally regulated. Specifically, down-regulation of *FTH1* (Table III S) is necessary for the ability of *myc* to induce cellular transformation. *SCHIP1* and members of the 14–3–3 protein family (*YWHAH* and *YWHAH*) react with merlin (Tables II and III S). *EB1* (Table V S) and *TTC2* (Table III S) interact with adenomatous polyposis coli and neurofibromin gene, respectively.

The enhanced expression of *ATWP* may be in response to a higher energy requirement of the tumor cells (Table IV S). Interestingly, channels that conduct chloride, potassium, calcium, sodium, and bicarbonate and proteins that bind and

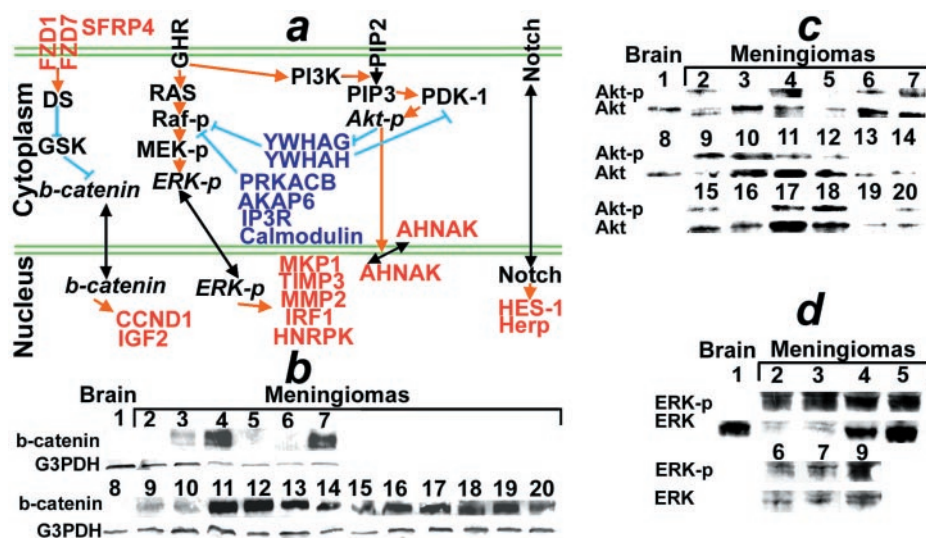


FIG. 2. The discovered differentially expressed genes predict activation of signaling pathways. *a*, a schematic portraying how some of the differentially expressed genes fit into the Wnt, MAPK, PI3K, and notch signaling pathways. Genes that are up-regulated or down-regulated in meningiomas as compared with normal brain are shown in red and blue, respectively. Inhibitory and stimulatory (facilitating) "interactions" are depicted as cyan and orange, respectively. Orange arrows in the nuclear compartment imply induction of transcription. Double arrows indicate translocation between cellular compartments. Double green lines depict the nuclear and plasma membranes. DS, disheveled; GHR, growth hormone receptor; MEK, dual-specificity kinase; ERK, MAP kinase; -p, phosphorylated protein; PI3K, phosphoinositide 3-kinase; PDK-1, phosphoinositide-dependent kinase 1; PIP2, phosphatidylinositol-4,5-bisphosphate; PIP3, phosphatidylinositol-3,4,5-triphosphate; Akt, protein kinase B. Panels *b*–*d* confirm the activation of the Wnt, MAP kinase, and PI3K signaling pathways in meningiomas. Western analysis of extracts from normal brain (lanes 1 and 8) and 18 meningiomas (lanes 2–7 and 9–20) reacted with antibodies against β -catenin (*b*), glyceraldehydes-3-phosphate dehydrogenase (G3PDH, *b*), Akt (*c*), phospho-Akt (Ser-473, Akt-p, *c*), p44/42 MAP kinase (ERK, *d*), and phospho-p44/p42 Map kinase (Thr-202/Tyr-204, ERK-p, *d*).

regulate these channels are transcriptionally regulated in meningiomas (Table IV S). The findings link ion homeostasis to the biology and phenotypes of meningiomas. The expression of molecules involved in cell-cell and cell-matrix interactions (STAB2 and EMP1), gap junctions (connexin 26), basal lamina (LAMB1 and LAMB2), and desmosomes (desmoplakin and DSG1) are higher in meningiomas than brain.

The cytoskeleton of meningiomas is likely to contain higher amounts of keratins 7 and 8 but lower amounts of tubulin than brain (Table V S). In addition, the expression levels of the actin-binding proteins T-plastin (PLS3), ARHA, ARHC, SDC2, TPM1, EPLIN- β , DMD, CALD1 (Table V S), and AHNAK (Table II S) are higher, whereas the expression levels of molecules that regulate microtubules dynamics, including EB1 and STMN1, are lower in meningiomas than brain (Table V S). Syntenin, which couples the transmembrane proteoglycans syndecans to cytoskeletal proteins, is down-regulated. PNUTL1 and SEPT, members of the septin family that regulate cell division and interact with actin and microtubules, are also down-regulated.

Meningiomas often produce cartilage and ectopic calcification; the tumors show higher expression of the types of collagen shown in Table VI S than brain. Up-regulation of the proteoglycans fibromodulin and decorin and loss of Rore2 suggest deposition of "atypical" cartilage. The extracellular matrix of meningiomas seems to be undergoing active remodeling as evidenced by higher expression of cathepsin L, MMP2, TIMP3, and lower expression of testican 3 than brain (Table VI S). Cathepsin L and matrix metalloproteinases 2 break down the extracellular matrix; the latter also degrades type IV collagen. Testican 3 regulates the activation of matrix metalloproteinases, and TIMP3 prevents the degradation of proteoglycans.

Ectopic bone formation is mediated by 1) enhanced expression of genes that induce and facilitate ectopic calcification, including CDH11, SLC26A2, SLC20A2, Endo180, OIF, SPARC, GDF11, and ALPL (Table VI S); 2) production of osteoprotegerin, a competitor that inhibits bone resorption by

RANKL; and 3) down-regulation of matrix Gla protein, an inhibitor of cartilage calcification.

Several hypoxia-inducible and/or angiogenesis-promoting genes are up-regulated in meningiomas, including endothelin receptors types A and B, placental growth factor (Table VII S), connective tissue growth factor (Table III S), fibronectin 1, matrix metalloproteinases 2, osteonectin (Table VI S), and aryl hydrocarbon receptor nuclelease translocator (Table III S). Pigment epithelium growth factor, a potent inhibitor of angiogenesis, is also up-regulated; the findings support the idea of Ohno-Matsui *et al.* (6) that angiogenesis is generated by disruption of a critical balance between pigment epithelium growth factor and angiogenesis-promoting molecules. Interestingly, meningiomas also appear to actively maintain a viable blood supply by producing molecules that prevent blood clotting. The latter include the vitamin K-dependent protein S (PROS1) and genes that regulate the complement cascade (Table VII S).

To survive within a host, the tumor needs protection from the immune response (Table VII S). Meningiomas appear to evade immunological surveillance by 1) regulating the classic and alternate complement cascade to escape from complement-mediated killing; 2) up-regulating matrix metalloproteinases 2 and the protease inhibitor SLP1 to dampen the local immune response; 3) down-regulating VAP1 and the cerebral cell adhesion molecule to block lymphocyte migration across the blood brain barrier; and 4) enhancing the expression of JAM2 to "seal" the blood brain barrier. In addition, PROL4 may contribute an "adaptive barrier function." Not unlike the genes shown in Tables I–VII S, the genes and ESTs of Tables VIII–XI S are also likely to play critical roles in creating the phenotypes of meningiomas (see Supplement). Others have reported expression states in meningiomas that are consistent with our data (7). Some of the expression states in Tables I–XI S, including the ESTs, have also been reported in gliomas by this laboratory (8). Eleven ESTs are down-regulated in both gliomas and meningiomas and four ESTs are up-regulated in both tumors as

compared with brain; linking ESTs to tumors and their genetic networks is an important step in investigating their functions.

The results demonstrate the relevance of genomic expression discovery to functional genomics; specifically, genomic expression discovery predicts activation of signaling pathways and uncovers unbalanced opposing functions behind specific phenotypes. The findings suggest the principles of multiplicity and balanced genetic expression. Multiplicity is apparent because of the multifunctionality of single genes and because a given phenotype is caused not by a single molecule but rather by up-regulating several genes that promote a desirable "aberrant" function and by down-regulating a number of genes that prevent it. Thus, a "normal" biological phenotype seems to be created, maintained, and controlled by a tight balancing of opposing molecular functions. Meningiomas disturb this balanced expression to promote their phenotypes. Known genetic functions and interactions draw multiple stimulatory and inhibitory connections (Fig. 2 and supplemental material). Uncovering the diverse functions of the individual genes including the ESTs seems necessary for configuring a two-dimensional scene of genetic interactions; however, it may not be sufficient for engendering an understanding of how the genes work together to make the totality. A mathematical simulation of the dynamics may enhance our ability to see the system as a whole

and to understand how these 364 genes create the biological phenotypes (1, 9). The findings demonstrate the significance and cost effectiveness of discovering highly specific states of genetic expression.

Acknowledgment—We thank R. Rosenberg for a critical review.

REFERENCES

1. Csete, M. E., and Doyle, J. C. (2002) *Science* **295**, 1664–1669
2. Ayerbe, J., Lobato, R. D., de la Cruz, J., Alday, R., Rivas, J. J., Gomez, P. A., and Cabrera, A. (1999) *Acta Neurochir.* **141**, 921–932
3. James, M. F., Manchanda, N., Gonzalez-Agosti, C., Hartwig, J. H., and Ramesh, V. (2002) *Biochem. J.* **356**, 377–386
4. Antinheimo, J., Sankila, R., Carpen, O., Pukkala, E., Sainio, M., and Jaaskelainen, J. (2002) *Neurology* **54**, 71–76
5. Langford, L. A., Piatyszek, M. A., Xu, R., Schold, S. C., Jr., Wright, W. E., and Shay, J. W. (1997) *Hum. Pathol.* **28**, 416–420
6. Ohno-Matsui, K., Morita, I., Tombran-Tink, J., Mrazek, D., Onodera, M., Uetama, T., Hayano, M., and Mochizuki, M. (2001) *J. Cell. Physiol.* **189**, 323–333
7. Watson, M. A., Peterson, K., Chicoine, M. R., Kleinschmidt-DeMasters, B. K., Brown, H. G., and Perry, A. (2002) *Am. J. Path.* **161**, 665–672
8. Fathallah-Shaykh, H., Rigen, M., Zhao, L.-J., Bansal, K., He, B., Engelhard, H., Cerullo, L., Von Roenn, K., Byrne, R., Munoz, L., Rosseau, G., Glick, R., Lichter, T., and DiSavino, E. (2002) *Oncogene* **21**, 7164–7174
9. Davidson, E. H., Rast, J. P., Oliveri, P., Ransick, A., Caletani, C., Yuh, C. H., Minokawa, T., Amore, G., Hinman, V., Arenas-Mena, C., Otim, O., Brown, C. T., Livi, C. B., Lee, P. Y., Revilla, R., Rust, A. G., Pan, Z., Schilstra, M. J., Clarke, P. J., Amone, M. L., Rowen, L., Cameron, R. A., McClay, D. R., Hood, L., and Bolouri, H. (2002) *Science* **295**, 1669–1678